Microsystem Technologies (2019) 25:1235–1241
https://doi.org/10.1007/s00542-018-4226-2

TECHNICAL PAPER

Fabrication of high fill-factor aspheric microlens array by dose-modulated lithography and low temperature thermal reflow

Junjie Zhu[1] · Mujun Li[1] · Jinfeng Qiu[1] · Huichun Ye[2]

Received: 27 May 2018 / Accepted: 12 November 2018 / Published online: 19 November 2018

Abstract
A cost-effective fabrication method for high quality and high fill-factor aspheric microlens arrays (MLAs) is developed. In this method, the complex shape of aspheric microlens is pre-modeled via dose modulation in a digital micromirror device (DMD) based maskless projection lithography system. Digital masks for several bottom layers are replaced from circle to hexagon for the purpose of enhancing the fill-factor of MLAs, then a low temperature thermal reflow process is conducted, after which the average surface roughness of microlens is improved to $\sim$ 0.427 nm while the pre-modeled profile keeps unchanged. Experimental results show that the fabricated aspheric MLAs have almost 100% fill-factor, high shape accuracy and high surface quality. The presented method may provide a promising approach for rapidly fabricating high quality and high fill-factor aspheric microlens in a simple and low-cost way.

1 Introduction

Recently, microlens arrays (MLAs) have attracted intensive attention and have been widely used in optical applications, such as fiber coupling (Hahn et al. 2010), optical loss reduction (Chen et al. 2015), optical sensors (Vekshin et al. 2010), imaging (Li and Allen 2012) and light diffusers (Wu et al. 2008), etc. For those optical systems, profile is one of the critical parameters that influence the MLAs performance. MLAs of aspheric profile have several benefits compared to MLAs of spherical profile, such as making the optical system much smaller, lighter, lower cost and better performance (Wu et al. 2009). The other critical parameter affecting the MLAs performance is the fill-factor, which is defined as the percentage of lens area to the total area (Yang et al. 2004). To make full use of the light, the fill-factor should be as close to 100% as possible. However, it is very difficult to achieve such a high fill-factor. Normally for round microlenses in an orthogonally arranged array, the maximum fill factor (assuming there are no gap between the lenses) is 78%. While in a hexagonally arranged array, the fill-factor can be larger (about 90%) (Lin et al. 2003).

Various techniques have been put forward for the fabrication of MLAs, including femtosecond laser micro-nanofabrication (Wu et al. 2009), the ultra-precision diamond cutting (Zhu et al. 2015), thermal reflow (Chung and Hong 2007) and DMD-based maskless lithography (Huang et al. 2018), etc. Among all these methods, DMD-based maskless lithography has its unique advantages for its real-time, maskless and cost-effective process. In our previous work, a single scan strategy based on the spatial distribution of exposure dose for 3D microstructures was developed to fabricate MLAs via equal-arc-mean slicing method (Huang et al. 2017). This dose-modulate method can fabricate 3D microstructures layer by layer and the exposure dose of each layer is determined by it's height. With this strategy, complex microstructures such as microlenses of ellipsoid profile or parabolic profile could be generated with high profile accuracy. However, the surface quality of MLAs is severely limited because the stairs between adjacent layers will form a discontinuous and unsmooth profile. In addition, the fill-factor of MLAs is hard to reach 100% through DMD-based maskless lithography. Traditional thermal reflow (Lin et al. 2003) is usually used to improve the surface quality of MLAs or increase the fill-factor of MLAs. However, when the fill-factor of MLAs is approaching 100% traditional thermal reflow may result in

✉ Mujun Li
lmn@ustc.edu.cn

[1] Department of Precision Machinery and Precision Instrumentation, University of Science and Technology of China, Hefei, Anhui 230026, People's Republic of China

[2] Engineering Practice Center, University of Science and Technology of China, Hefei, Anhui 230026, People's Republic of China

merging of lenses by experiment result. Moreover, the diameter and height of microlens will change during the traditional thermal reflow process, which may make the profile of microlens difficult to control (Park et al. 2014).

In this work a cost-effective method is introduced combining dose-modulated DMD based lithography, digital masks replacement and low temperature thermal reflow to fabricate high quality aspheric MLAs of 100% fill-factor. Firstly, digital masks are calculated by equal-arc-mean slicing method. Secondly, the digital masks of several bottom layers are replaced with hexagonal array to increase fill-factor of MLAs (Zhong et al. 2017). Thirdly, a low temperature thermal reflow process is conducted under a temperature which is relatively lower than the glass transition temperature (Tg) to obtain accurate microlens profile with smooth surface and avoid the merging of lenses. Results show that the digital masks replacement can enhance the fill-factor to almost 100%. In addition, low temperature thermal reflow can avoid merging of lenses, keep the profile of microlens unchanged and improve the surface quality. In the previous work of our lab, the average surface roughness (Ra) of microlens's top surface is ~ 38.4 nm before reflow (Huang et al. 2018). The Ra is measured at the microlens top surface after low temperature thermal reflow, which is improved to ~ 0.427 nm. The surface quality of MLAs is improved significantly after reflow.

2 Experimental setup

The schematic diagram of the system is shown in Fig. 1. A mercury lamp (OmniCureTM S1500) is used as a light source which is filtered at a wavelength of 365 nm. Then a high power fiber light guide and an adjustable collimating adapter are used to make the light homogenized and collimated. The DMD (Texas Instruments Co. America) consisted of an array of 1024 × 768 micromirrors works as a physical mask by generating a dynamic mask in real time. Through the DMD, the illumination light can be modulated, and then projected onto the 3D motorized linear stage (Bocic Co., China) through the objective lens (CFI Plan Flour × 4, Nikon Co. Japan). The tube lens helps to correct the chromatic aberration of the illumination light and improve the imaging quality. Defocus phenomenon can be effectively avoid and large area exposure can be realized through the 3D motorized linear stage.

The fabrication process of high quality MLAs is illustrated in Fig. 2. First, the AZ P4620 (a positive photoresist from Clariant) is spin coated on a glass substrate at 3000 rpm, which can obtain a photoresist layer of about 10 µm. Then the sample is prebaked on a hotplate at 100 °C for 6 min, as shown in Fig. 2a. Next, UV exposure is conducted with the DMD-based maskless lithography system, as shown in Fig. 2b. The intensity of UV light was 10 mW/cm^2. Then the sample is developed in AZ 400 K alkaline solution (AZ 400 K: DI water = 1:4) for 3 min and finally rinsed in deionized water for a few seconds, initial microlens can be obtained as shown in Fig. 2c. The magnified image of a single microlens after development is shown in Fig. 2f. To ensure the quality of surface profile of microlens and keep the profile unchanged, a relative low temperature is used in the thermal reflow process. The sample is putted on a hotplate at 110 °C for 5 min which is lower than the Tg of AZ P4620 (115 °C), as shown in Fig. 2d and after reflow the surface quality of microlens will be improved significantly, as shown in Fig. 2e.

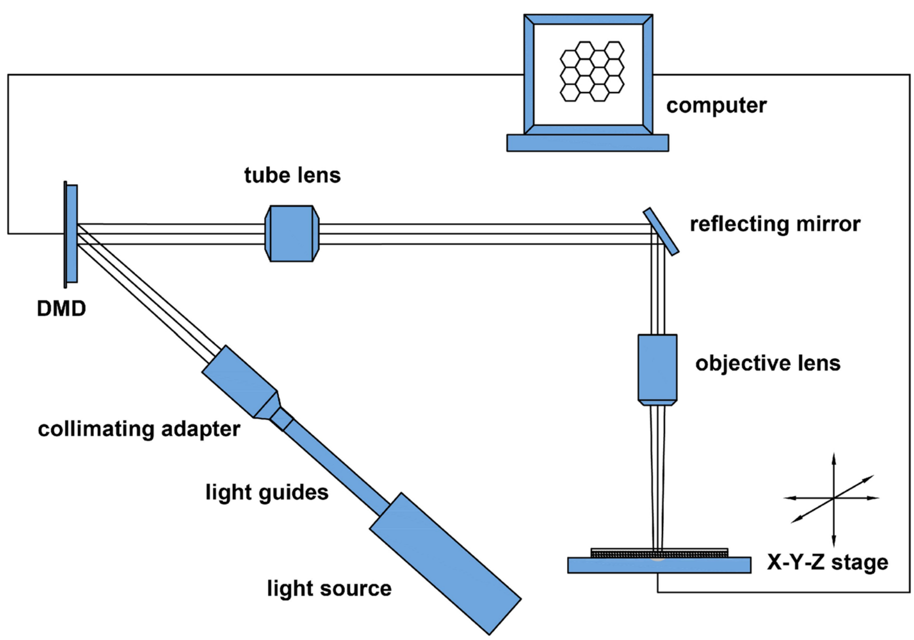

Fig. 1 Schematic diagram of the DMD-based maskless lithography system

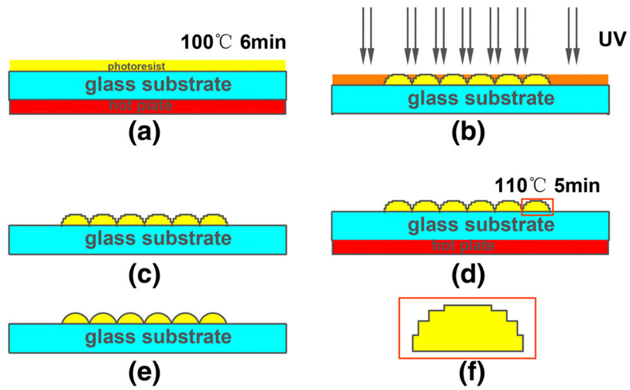

Fig. 2 Schematic diagram of the fabrication process of a high quality MLA

In order to process aspheric MLAs, the equal-arc-mean slicing method is applied as shown in Fig. 3. The design profile of ellipsoid microlens is $(x^2 + y^2)/R^2 + z^2/H^2 = 1$. In our DMD-based maskless lithography system, a pixel in digital mask is approximately 1.84 µm on the image plane. The parameter of R is set to 25 pixels in digital mask (about 46 µm in the image plane). The parameter of H is 9.5 µm because the thickness of the photoresist is about 9.5 µm. So the design profile is $(x^2 + y^2)/46^2 + z^2/9.5^2 = 1$. According to the equal-arc-mean slicing method, the design profile with height H is divided into 16 segments, each of which has an equal arc-length of ΔL. The radius of each layer r_i and height of each layer h_i are calculated, as shown in Table 1.

The positive photoresist AZ P4620 is chosen in our experiment. For AZ P4620, the development depth $h(x, y)$ of photoresist and the exposure dose $E(x, y)$ are assumed to be a logarithmic relationship: $h(x, y) = H\gamma[\ln(E(x, y)) - \ln(E_{th})]$. E_{th} and γ are the exposure threshold and the value of contrast, respectively, and H is the total height of resulted profile. According to our lab's previous work and

Fig. 3 Schematic diagram of equal-arc-mean slicing

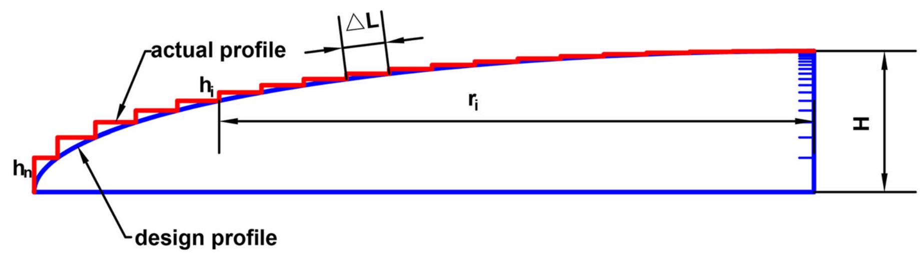

Table 1 The radius and height of i'th layer

i'th layer	1	2	3	4	5	6	7	8
r_i (µm)	3.01	6.02	9.03	12.02	15.03	18.03	21.03	24.02
h_i (µm)	0.02	0.06	0.10	0.15	0.19	0.24	0.29	0.35
i'th layer	9	10	11	12	13	14	15	16
r_i (µm)	27.0	29.98	32.95	35.88	38.79	41.63	44.31	46
h_i (µm)	0.41	0.48	0.58	0.69	0.83	1.07	1.49	2.55

Fig. 4 **a** Digital masks before replacement, **b** digital masks after replacement

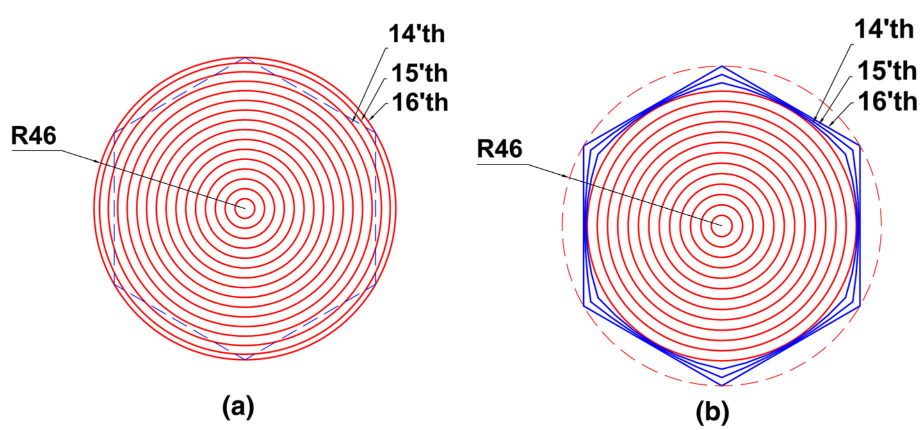

our calculation, E_{th} = 35.8845 mJ/cm^2 and γ = 0.4884 can be obtained (Huang et al. 2018). Then the exposure dose of each layer can be determined according to the height of each layer.

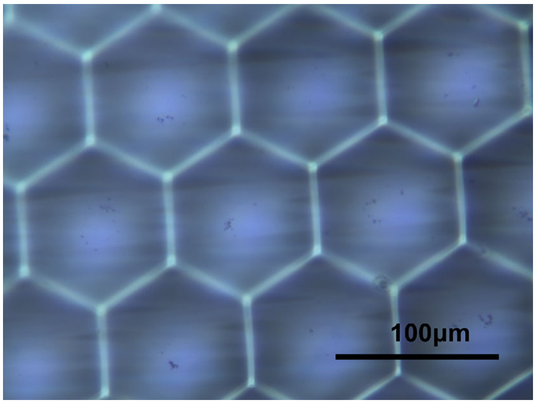

Fig. 5 Optical microscope image of part of fabricated microlens array

The digital masks of each layer are determined as illustrated in Fig. 4a. However, the radiuses of 14'th, 15'th and 16'th digital masks are beyond the designed hexagon through calculation. So the digital masks of the 14'th, 15'th and 16'th layers at the bottom of microlens should be replaced. Figure 4b shows the digital masks after replacement. The bases of microlenses are changed into hexagon and the microlenses are hexagonally arranged, therefore the fill-factor can be enhanced to 100% theoretically. According to experimental results, a small gap is necessary between microlenses when the thermal reflow process is conducted. The gap is determined as 4 μm through experimental tests.

3 Results and discussion

With the fabrication method mentioned above, experiments and measurements are conducted. Firstly, the digital masks of aspheric MLAs are calculated by the equal-arc-mean

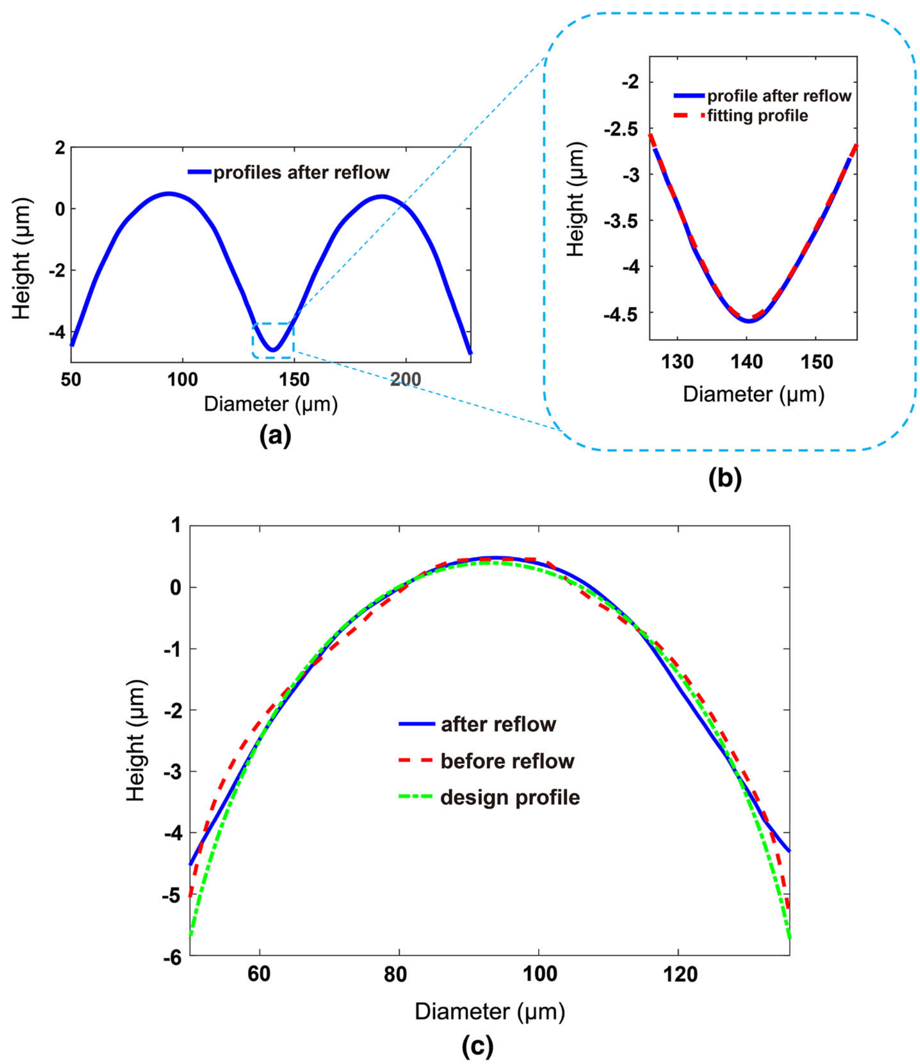

Fig. 6 **a** Profiles of cross microlenses after low-temperature thermal reflow, **b** profiles of the intersection, **c** comparison of microlens profile before and after thermal reflow relative to the design profile

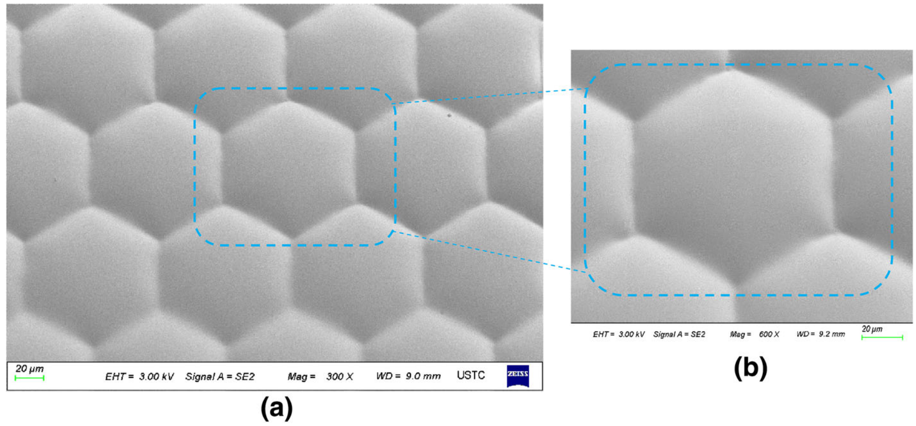

Fig. 7 The SEM images of the fabricated microlens array: **a** part of microlens array, **b** enlarged view of microlenses

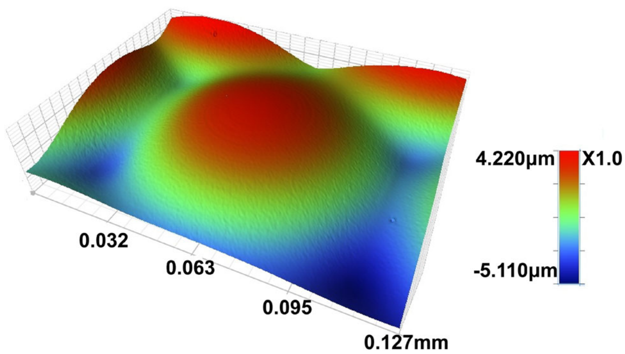

Fig. 8 3D profile of microlenses measured by 3D optical profiler

slicing method. Secondly, the exposure of each layer is determined and the digital masks of the bottom layers are replaced through our calculation. Thirdly, the exposure process is conducted, after which a low temperature thermal reflow process for the sample is carried out.

The optical microscope image of part of aspheric microlens array after reflow is shown in Fig. 5. The area of microlens array is about 1.4 × 1.4 mm. It can be seen that the microlenses are orderly arranged and have clear profile. We can also learn that there is no merging between microlenes through our method and the edges of microlenses are fairly clear.

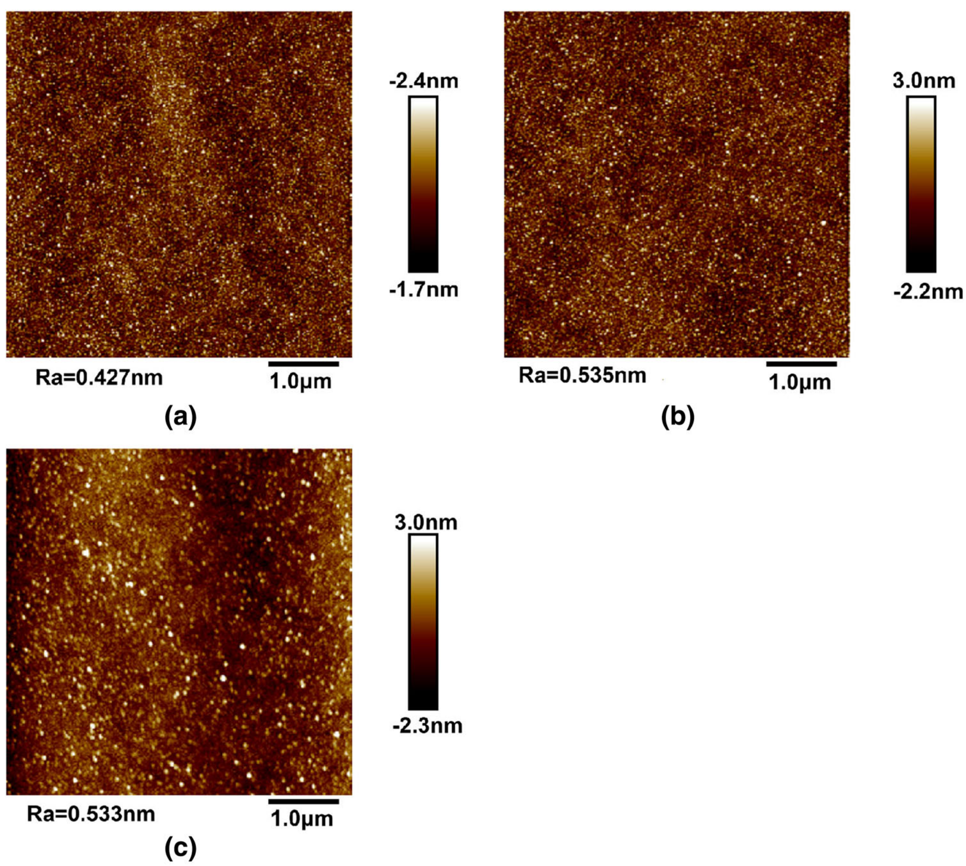

Fig. 9 The AFM images of the fabricated microlens after reflow: **a** the top area, **b** the middle area, **c** the bottom area

The profiles are measured by the Bruker Stylus Profiler (Dektak XT) as shown in Fig. 6. Figure 6a shows the profiles of microlenses after low-temperature thermal reflow. It can be seen that the profiles of microlenses are quite smooth and there is no merging between microlenses. Figure 6b shows the intersection of the adjacent microlenses. The solid line is the microlens profile and the dashed line is the elliptic curve that is fitted with the least square method. It can be learned that the intersection of the microlenses is also smooth and very approximate to the elliptic profile, which indicates that almost 100% fill-factor is successfully achieved. Figure 6c shows the measured results of microlens profile before and after low-temperature thermal reflow, respectively. The red line is the profile before reflow and the blue line is the profile after reflow. It can be seen that these two profiles are very close and they are both coincident with the design profile (the green line), which means that the profile has a high fidelity and remains unchanged after reflow.

Figure 7a shows the scanning electron microscope (SEM) image of part of the microlens array. It can be seen that the uniformity of microlenses is very good and the fill-factor reaches 100%. Figure 7b is the enlarged view of the microlenses, which shows that the microlens has a good shape and high surface quality.

Figure 8 shows the 3D profile of the fabricated microlens measured by 3D optical profiler (Wyko NT1100, America). It can be seen that the microlens has smooth surface and good aspheric profile, and the connection area between microlenes is smooth too, which means that there is no merging between microlenes and the fill-factor reaches 100% actually.

The roughness of the surface is measured by the atomic force microscope (AFM), as shown in Fig. 9. The average surface roughness (Ra) is measured at a 5 by 5 μm measurement area on the top area, middle area and bottom area respectively. The average surface roughness (Ra) is ∼ 0.427 nm on the top area, ∼ 0.535 nm on the middle area and ∼ 0.533 nm on the bottom area as shown in Fig. 9a–c. It means that the entire surface of microlens is quite smooth after reflow.

To investigate the focusing capability of the fabricated microlens arrays, optical testing is conducted using an optical testing system, as shown in Fig. 10a. In the experiment, the fabricated microlens array is placed on a linear translation stage, and a CCD camera is used to monitor the light passing through the microlens array and microscope system. An array of bright focal spots is observed through the microscope system, as shown in Fig. 10b. The focal spots are quite sharp and uniform.

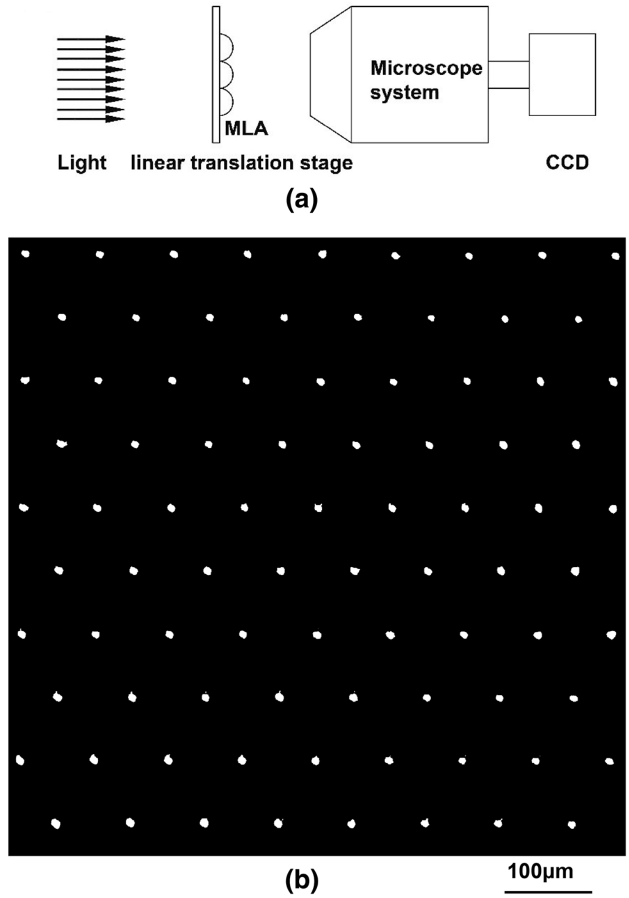

Fig. 10 Optical testing. **a** Optical testing system, **b** focal spot image of the fabricated microlens array

4 Conclusions

A cost-effective method for fabricating high fill-factor microlens array with high surface quality is proposed using the DMD-based lithography and low temperature thermal reflow. An improved slicing method called equal-arc-mean method and digital mask replacement are employed to obtain an accurate profile and enhance the fill-factor of microlens array. Afterwards, a low temperature thermal reflow process is conducted to smooth the surface of microlenses. Experimental results show that 100% fill-factor aspheric microlens array with good shape and high surface quality with roughness of ∼ 0.427 nm is achieved. The proposed method may provide a promising way for the fabrication of high fill-factor aspheric microlens array with variable curvature or complex shape. It's expected that the method will find a broad range of potential applications of different optical fields such as optical signal processing system and optical communication system.

Acknowledgements This work was supported by funding from the National Natural Science Foundation of China (Grant No. 51475442), the Fundamental Research Funds for the Central Universities, and partially carried out at the University of Science and Technology of China Center for Micro and Nanoscale Research and Fabrication.

References

Chen Y et al (2015) Reducing optical losses in organic solar cells using microlens arrays: theoretical and experimental investigation of microlens dimensions. Phys Chem Chem Phys 17(5):3723–3730

Chung CK, Hong YZ (2007) Fabrication and analysis of the reflowed microlens arrays using JSR THB-130 N photoresist with different heat treatments. Microsyst Technol 13(5–6):523–530

Hahn DV et al (2010) Fiber optic bundle array wide field-of-view optical receiver for free space optical communications. Opt Lett 35(21):3559–3561

Huang S et al (2017) Improved slicing strategy for digital micromirror device-based three-dimensional lithography with a single scan. Micro Nano Lett 12(1):49–52

Huang S et al (2018) Fabrication of high quality aspheric microlens array by dose-modulated lithography and surface thermal reflow. Opt Laser Technol 100:298–303

Li L, Allen YY (2012) Design and fabrication of a freeform microlens array for a compact large-field-of-view compound-eye camera. Appl Opt 51(12):1843–1852

Lin CP, Yang H, Chao CK (2003) Hexagonal microlens array modeling and fabrication using a thermal reflow process. J Micromech Microeng 13(5):775

Park MK et al (2014) Design and fabrication of multi-focusing microlens array with different numerical apertures by using thermal reflow method. J Opt Soc Korea 18(1):71–77

Vekshin MM et al (2010) Glass microlens arrays for Shack-Hartmann wavefront sensors. Meas Sci Technol 21(5):3–143

Wu CY, Chiang TH, Hsu CC (2008) Fabrication of microlens array diffuser films with controllable haze distribution by combination of breath figures and replica molding methods. Opt Express 16(24):19978–19986

Wu D et al (2009) 100% fill-factor aspheric microlens arrays (AMLA) with sub-20-nm precision. IEEE Photonics Technol Lett 21(20):1535–1537

Yang H et al (2004) High fill-factor microlens array mold insert fabrication using a thermal reflow process. J Micromech Microeng 14(8):1197

Zhong K, Zhang H, Gao Y (2017) Fabrication of high fill-factor aspheric microlens array by digital maskless lithography. Optik-Int J Light Electron Opt 142:243–248

Zhu Z, To S, Zhang S (2015) Large-scale fabrication of micro-lens array by novel end-fly-cutting-servo diamond machining. Opt Express 23(16):20593–20604